



# Molecular Modeling of Protein Tyrosine Phosphatase 1B (PTP 1B) Inhibitors

V. Sreenivasa Murthy and Vithal M. Kulkarni\*

*Pharmaceutical Division, Department of Chemical Technology, University of Mumbai, Matunga, Mumbai 400 019, India*

Received 25 July 2001; accepted 17 September 2001

**Abstract**—Binding modes of a series of aryloxymethylphosphonates and monoanionic biosteres of phosphate group from a series of benzylic  $\alpha,\alpha$ -difluoro phosphate and its biosteres as protein tyrosine phosphatase 1B (PTP 1B) inhibitors have been identified by molecular modeling techniques. We have performed docking and molecular dynamics simulations of these inhibitors with PTP 1B enzyme. The initial conformation of the inhibitors for docking was obtained from simulated annealing technique. Solvent accessible surface area calculations suggested that active site of PTP 1B is highly hydrophobic. The results indicate that for aryloxy-methylphosphonates, in addition to hydrogen bonding interactions, Tyr46, Arg47, Asp48, Val49, Glu115, Lys116, Lys120 amino acid residues of PTP 1B are responsible for governing inhibitor potency of the compounds. The sulfonate and tetrazole functional groups have been identified as effective monoanionic biosteres of phosphate group and biphenyl ring system due to its favorable interactions with Glu115, Lys116, Lys120 residues of PTP 1B found to be more suitable aromatic functionality than naphthalene ring system for benzylic  $\alpha,\alpha$ -difluoro phosphate and its biosteres. The information generated from the present study should be useful in the design of more potent PTP 1B inhibitors as anti diabetic agents. © 2002 Elsevier Science Ltd. All rights reserved.

## Introduction

Resistance to the biological actions of insulin in its target tissues is a major feature of the patho-physiology in human obesity and in non-insulin dependent diabetes mellitus (NIDDM). Tyrosine phosphorylation of specific intracellular proteins controlled by the actions of protein tyrosine kinases (PTKs) and protein tyrosine phosphatases (PTPs) is recognized as a key process by which a number of polypeptide hormones and growth factors transduce and co-ordinate their biological effects in vivo.<sup>1</sup> Recent insights into the mechanism of insulin action have demonstrated that reversible tyrosine phosphorylation of the insulin receptor and its cellular substrate proteins play a central role in the mechanism of insulin action.<sup>2</sup> Biochemical and cellular studies have provided evidences that PTPs have an important role in the regulation of insulin signal transduction.<sup>3</sup>

Protein tyrosine phosphatase 1B (PTP 1B), a cytosolic PTP play a major role in regulation of insulin sensitivity and dephosphorylation of the insulin receptor. PTP 1B has been implicated as negative regulator of insulin receptor signaling.<sup>4,5</sup> Clinical studies have found a correlation between insulin resistance states and levels of PTP 1B expression in muscle and adipose tissues, suggesting that PTP 1B has a major role in the insulin resistance associated with obesity and NIDDM.<sup>6,7</sup> A recent pivotal PTP 1B knock out study revealed that mice lacking functional PTP 1B exhibit increased sensitivity toward insulin resistance and are resistant to obesity.<sup>8</sup> All these results establish a direct role for PTP 1B in down regulating the insulin functions. Hence potent, orally active and selective PTP 1B inhibitors could be potential pharmacological agents for the treatment of obesity and NIDDM.

The phosphoryl group and amino acid residues flanking the phosphotyrosyl (pTyr) residue contribute to high affinity substrate binding by PTPs. pTyr residues themselves are not ideally suited for inhibitor development due to liability of phosphate esters to hydrolysis by cellular phosphatases. Incorporation of non-hydrolyzable phosphate mimetic such as phosphonomethylphenylalanine (pmp), phosphonodifluoromethylphenylalanine (F<sub>2</sub>pmp), into a specific optimal peptide template resulted

\*Corresponding author. Tel.: +91-22-414-5614; fax: +91-22-414-5614; e-mail: vithal@biogate.com, vmk@pharma.udct.ernet.in

in the development of potent and selective PTP 1B inhibitors.<sup>9</sup> Although these peptide inhibitors are most potent, competitive and selective PTP 1B inhibitors, difficulties of cell membrane transport and the fact that they are peptide phosphonates make them less desirable as drug candidates. It has been observed that simple aryl phosphonates such as p-nitrophenylphosphate are hydrolyzed quite efficiently by tyrosine phosphatases.<sup>10</sup> Removal of peptide portion and incorporation of difluorophosphonomethyl moiety onto a naphthalene ring system resulted in quite potent PTP 1B inhibitor.<sup>11</sup> But these aryl phosphonates are inefficient in crossing cell membrane and unstable in vivo because of highly polar nature of dianionic phosphate group. It is evident from literature that monoanionic and dianionic forms of phosphate binds PTP 1B with equal efficiency.<sup>12</sup> Hence elucidation of binding modes of aryl phosphonates and identification of effective mono anionic biosteres of phosphate group may be helpful in design of PTP 1B inhibitors.

Ligand–receptor interactions, which are characterized explicitly, lead to identification of mechanistically relevant reactivity parameters, which are modulators of activity for a series of inhibitors and help in design of enzyme inhibitors as drugs. Molecular mechanics based methods involving docking studies and molecular dynamics simulations (MD) have been used to study the binding orientations and prediction of binding affinities. Such studies have been applied in case of acetylcholinesterase inhibitors,<sup>13</sup> interleukin 1 $\beta$ -converting enzyme (ICE) inhibitors,<sup>14</sup> protein kinase inhibitors such as staurosporine.<sup>15</sup> In the case of herpes simplex virus thymidine kinase inhibitors,<sup>16</sup> these studies have been used to predict binding affinities quantitatively. Docking and molecular dynamics simulations have been used to reveal the structural factors responsible for selectivity of inhibitors between *Candida albicans* fungal and human DHFR.<sup>17</sup>

Among the aryl phosphonates, aryloxymethylphosphonates<sup>18</sup> possess structurally different functionalities. We have selected this series to elucidate their binding modes with PTP 1B by docking and MD simulations and to derive structure–activity relationship. In order to find out effective monoanionic phosphate biosteres, docking and MD simulations were performed on a series of benzylic  $\alpha,\alpha$ -difluorophosphate and its monoanionic biosteres such as  $\alpha,\alpha$ -difluorosulfonate (CF<sub>2</sub>-sulfonate),  $\alpha,\alpha$ -difluorotetrazole (CF<sub>2</sub>-tetrazole),  $\alpha,\alpha$ -difluorocarboxylate (CF<sub>2</sub>-carboxylate).<sup>19</sup>

## Results

A series of aryloxymethylphosphonates<sup>18</sup> with  $K_i$  (mM) were selected to elucidate their binding modes and to explain the structure–activity data by docking and MD simulations. A series of benzylic  $\alpha,\alpha$ -difluoro benzyl phosphate and its biosteres<sup>19</sup> with IC<sub>50</sub> ( $\mu$ M) were selected in an attempt to find out effective monoanionic phosphate biostere through docking and MD simulations. All the compounds were constructed using stan-

dard geometry and standard bond lengths. Lowest energy conformers were located by performing simulated annealing. These conformers were used for docking.

Trajectory data from MD simulations was analyzed on the basis of the following parameters:

- Hydrogen bonding interactions,
- Energy of binding,
- Rms deviation of the active site residues,
- Orientation of the inhibitor within the active site,
- Other interactions such as aromatic  $\pi$ – $\pi$  stacking interactions, hydrophobic interactions.

The hallmark of PTP family of enzymes is the PTPs' signature motif, (H/V)CX5R (S/T); housed in the catalytic domain.<sup>20</sup> Inhibition of PTP 1B is known to be mediated by hydrogen bonding interactions between inhibitors and signature motif residues of the active site (Cys215, Ser216, Ala217, Gly218, Ile219, Gly220, Arg221). Literature suggests that these hydrogen bonds are the main recognition elements for PTP 1B–ligand interactions.<sup>21</sup> Taking into consideration of this factor we have used hydrogen bond interactions as one of the criteria for the analysis of MD trajectories. Energy of binding was calculated for each compound after minimization of the selected trajectory frames, as the difference between the energy of the complex and individual energies of the enzyme and compound.<sup>22</sup>

$$E_{\text{binding}} = E_{\text{complex}} - (E_{\text{enzyme}} + E_{\text{compound}})$$

Molecular docking and dynamics were performed on each compound with the enzyme. The orientation for each compound discussed here represents the best orientation and is the representative of all possible interactions within the active site.

## Aryloxymethylphosphonates

### Compound 1

Compound 1 (Table 1) binds to PTP 1B active site by hydrophobic  $\pi$ – $\pi$  stack interactions of phenyl ring with Tyr46 and Phe182, van der Waals contacts with aliphatic side chains of Ala217, Ile219, Gly220, Val49, and polar interaction with Gln262. The oxymethylphosphonate group form hydrogen bonds with signature motif residues. The guanidium group of Arg221 forms hydrogen bond with P=O and with one of the negatively charged oxygen atoms O<sub>a</sub><sup>–</sup> of phosphonate group. Amide proton of Gly220 forms hydrogen bond with second negatively charged oxygen atom O<sub>b</sub><sup>–</sup> of oxymethylphosphonate group. There is a charged interaction between guanidium side chain of Arg221 and oxymethylphosphonate group of compound 1. These interactions results in a favorable orientation of the compound within the active site with binding energy of –21.677 kcal/mol.

## Compound 2

Compound **2** (Table 1) possesses a propionate group at C<sub>4</sub> position on the phenyl ring and exhibits 3-fold more inhibitor potency than compound **1**. This compound maintained hydrophobic interactions, van der Waals contacts, and charged interactions same as that of compound **1**. The guanidinium group of Arg221 forms two hydrogen bonds with P=O and O<sub>a</sub><sup>-</sup>, amide proton of Gly220 with O<sub>b</sub><sup>-</sup>, Ser216 side chain-OH with etherial oxygen atom of oxy methyl phosphonate group.

The propionate group of compound **2** is oriented toward Lys120 residue. This resulted in strong charged interaction between Lys120 side chain NH<sub>3</sub><sup>+</sup> group and carboxylate anion of compound **2**. Additional hydrogen bonding interaction of O<sub>c</sub><sup>-</sup> with NH<sub>3</sub><sup>+</sup> of Lys120, van der Waals contacts with side chain of Lys116, Lys120 makes this compound three fold more potent than compound **1** with binding energy of -54.110 kcal/mol. The charged interaction, van der Waals contacts, and hydrogen bonding interactions of propionate group contributed to enhanced inhibitory potency of compound **2**.

## Compound 3

Figure 1 is the docking model of compound **3** into the active site of PTP 1B. This compound is stabilized in the active site predominantly by hydrophobic interaction and hydrogen-bond binding. compound **3** (Table 1) belongs to bis (para-oxymethyl phosphonophenyl) methane. The phenyl ring (A) exhibited hydrophobic  $\pi$ - $\pi$  stacking interaction with Phe182, van der Waals contacts with aliphatic side chains of Ser216, Ala217 and Gly218. The oxymethylphosphonate group exhibits hydrogen bonding interactions as follows: the guanidinium group of Arg221 form hydrogen bonds with P=O, and O<sub>a</sub><sup>-</sup>, amide protons of Ser216, Gly218 with O<sub>b</sub><sup>-</sup>, amide proton of Ala217 with etherial oxygen of oxymethylphosphonate group (Fig. 2). There is a charged interaction between oxymethylphosphonate group and guanidinium group of Arg221. The methylene spacer connecting the two phenyloxymethylphosphonates exhibit hydrophobic contacts with Ala217.

The phenyl ring (B) with oxymethylphosphonate group occupied the hydrophobic pocket formed by Tyr46, Arg47, Asp48 and Val49 residues. This phenyl ring made hydrophobic  $\pi$ - $\pi$  stacking interaction with Tyr46, van der Waals contacts with side chain of Arg47, Asp48 and Val49. The P=O of oxymethylphosphonate group form two hydrogen bonds with amide protons of Arg47 and Asp48, O<sub>c</sub><sup>-</sup> with amide proton of Val49, amide proton of Asp48 with etherial oxygen. There is a charged interaction between oxymethylphosphonate group and guanidinium group of Arg47.

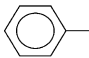
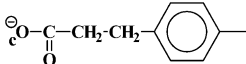
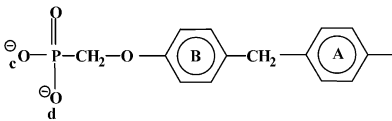
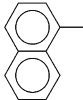
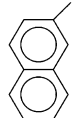
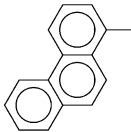
This compound binds PTP 1B enzyme with different binding orientation, with high total solvent-accessible surface area, total enclosed volume (Table 3) and possesses highest inhibitor potency among the series. Additional phenyloxymethylphosphonate group, which

binds effectively in the hydrophobic pocket formed by Tyr46, Arg47, Asp48 and Val49 with hydrophobic  $\pi$ - $\pi$  stack interactions, van der Waals contacts, hydrogen bonding interactions, and charged interaction contributed for the highest inhibitor potency and binding energy of -85.577 kcal/mol. Hence ligands with properly oriented functional groups, which can interact favorably with the residues present at the cleft of signature motif, show better inhibitory activity.

## Compound 4

Compound **4** (Table 1) incorporating naphthalene ring system as aryl substituent, showed three fold more inhibitory potency than compound **1**. In addition to the hydrophobic, van der Waals contacts, polar interactions of the phenyl ring of compound **4**, second phenyl ring of naphthalene ring system exhibits cationic  $\pi$  interactions with side chain NH<sub>3</sub><sup>+</sup> of Lys120, van der Waals contact with side chains of Glu115, Lys116, Lys120. The hydrogen bonding interactions of this compound are as follows: P=O forms two hydrogen bonds with guanidinium group of Arg221, O<sub>a</sub><sup>-</sup> with amide proton of Gly220, O<sub>b</sub><sup>-</sup> with amide proton of Ala217, etherial oxygen with side chain -OH of Ser216. The oxymethylphosphonate group of this compound exhibited charged interaction with guanidinium group of Arg221 residue.

**Table 1.** Structures and inhibition constants of aryloxymethylphosphonates with PTP 1B enzyme

$\text{Ar}-\text{O}-\text{CH}_2-\text{P}(\text{O})(\text{O}_a^-)(\text{O}_b^-)$		
Compd	Ar	PTP 1B K <sub>i</sub> (μM)
1		3.3 ± 0.2
2		1.1 ± 0.1
3		0.047 ± 0.005
4		1.3 ± 0.2
5		1.3 ± 0.1
6		0.41 ± 0.09

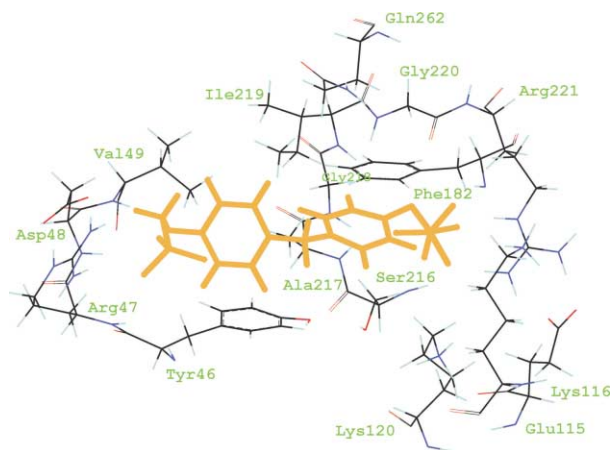
Additional cationic  $\pi$ -charged interactions with Lys120, van der Waals contacts with the side chains of Glu115, Lys116, Lys120, of the second phenyl ring of naphthalene makes this compound 3-fold more potent than compound **1** with binding energy of -48.147 kcal/mol.

### Compound 5

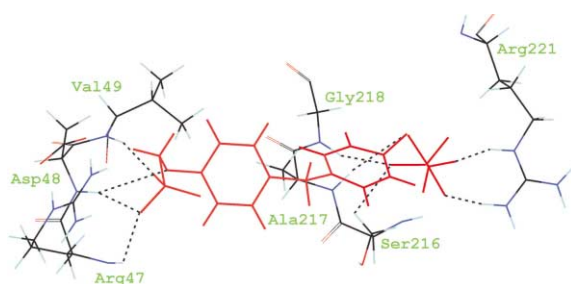
Shifting the position of attachment of oxymethylphosphonate group from first position to second in naphthalene ring does not effect the inhibitory potency of the compound **5** (Table 1). This indicates bulkier groups can be substituted to take the advantage of the hydrophobic pocket formed by Glu115, Lys116 and Lys120. This compound maintained all the hydrophobic interactions, van der Waals contacts and hydrogen bonding patterns same as that of compound **4** with binding energy of -49.498 kcal/mol. This compound possesses three fold more inhibitor potency than compound **1**.

### Compound 6

Compound **6** with phenanthrene ring system as aryl substituent of oxymethylphosphonate group exhibited binding orientation in the active site of PTP 1B as shown in the Figure 3. The phenanthrene ring system maximized interactions with Glu115, Lys116, Lys120 residues with binding energy of -52.682 kcal/mol. The phenanthrene ring system formed hydrophobic  $\pi$ - $\pi$  interactions with Tyr46 and Phe182, van der Waals contacts with side chains of Glu115, Lys116, Lys120,



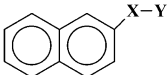
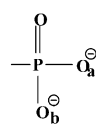
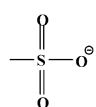
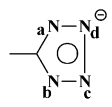
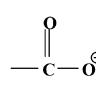
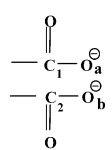
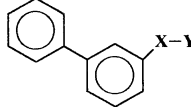
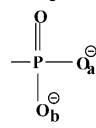
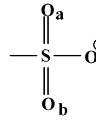
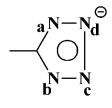
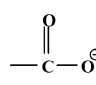
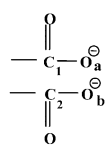
**Figure 1.** Binding orientation of compound **3** with PTP 1B active site residues (compound **3** showed in capped sticks).



**Figure 2.** Compound **3** with active site residues of PTP 1B with hydrogen bonds displayed.

Ile219, strong charged interactions with  $\text{NH}_3^+$  of Lys116, Lys120. The hydrogen bonding interactions of oxymethylphosphonate group are as follows: the guanidium group of Arg221 form hydrogen bond with  $\text{P}=\text{O}$ , amide proton of Gly220 with  $\text{O}_a^-$ , amide proton of Ala217 with  $\text{O}_b^-$ , -OH side chain of Ser216 with etherial oxygen of oxymethylphosphonate group of compound

**Table 2.** Structures and  $\text{IC}_{50}$  ( $\mu\text{M}$ ) values for benzylic  $\alpha,\alpha$ -difluorinated compounds with PTP 1B enzyme

			
Compd	X	Y	PTP 1B $\text{IC}_{50}$ ( $\mu\text{M}$ )
7	$-\text{CF}_2$		$35 \pm 5$
8	$-\text{CF}_2$		$175 \pm 10$
9	$-\text{CF}_2$		$230 \pm 12$
10	$-\text{CF}_2$		$640 \pm 18$
11	$-\text{OCF}$		$320 \pm 11$
			
12	$-\text{CF}_2$		$15 \pm 3$
13	$-\text{CF}_2$		$115 \pm 9$
14	$-\text{CF}_2$		$195 \pm 10$
15	$-\text{CF}_2$		$435 \pm 12$
16	$-\text{OCF}$		$250 \pm 10$

6. The side chain of Tyr46, Lys120 move toward phenanthrene ring system in order to maximize the interaction, which is evident from the rms value (Table 4). The third phenyl ring of compound **6** has additional cationic  $\pi$  interaction with side chain  $\text{NH}_3^+$  of Lys116 residue. The additional phenyl ring of compound **6** increased the total nonpolar surface area which may provide an additional entropic driving force on the order of 1.0 kcal/mol. This is evident from the high nonpolar surface area of this compound (Table 3). Hence compound **6** show 8-fold more inhibitor potency than compound **1**. These results are in consistent with the biological activity of this compound.

### Benzylic $\alpha,\alpha$ -Difluorophosphate and Biosteres

This series includes naphthyl  $\alpha,\alpha$ -difluorophosphate, biphenyl  $\alpha,\alpha$ -difluoro phosphate and biosteres. Docking and MD simulations were used to identify effective monoanionic phosphate biosteres that are more amenable to cellular studies than dianionic species.

### Naphthyl $\alpha,\alpha$ -Difluorophosphate and Biosteres

#### Compound 7

Compound **7** is naphthyl  $\alpha,\alpha$ -difluorophosphate (Table 2) with high activity among the series of naphthyl  $\alpha,\alpha$ -difluorophosphate and biosteres. The naphthalene ring of this compound forms aromatic  $\pi$ - $\pi$  interaction with Tyr46 and Phe182, Van der Waals contacts with aliphatic side chains of Ala217, Ile219, Lys120, Val49, and cationic  $\pi$  interaction with sidechain  $\text{NH}_3^+$  of Lys120. The difluorophosphate group forms hydrogen bonds with signature motif residues. Two fluorine atoms form hydrogen bond with amide protons of Phe182, Ala217, P=O with guanidium group of Arg221,  $\text{O}_a^-$  with amide proton of Gly218,  $\text{O}_b^-$  with amide proton of Gly220. There is charged interaction between phosphate group and guanidium group of Arg221. With all these interactions compound **7** binds to the active site of PTP 1B

with binding energy of -64.830 kcal/mol. This compound possesses high polar surface area (Table 3) among naphthyl  $\alpha,\alpha$ -difluorophosphate and biosteres.

#### Compound 8

Compound **8** is naphthyl  $\alpha,\alpha$ -difluorosulfonate (Table 2). The naphthalene ring maintained all the hydrophobic, van der Waals, polar interactions same as that of compound **7**. This compound exhibited hydrogen bond interactions as follows:  $\text{SO}_2$  of sulfonate group with guanidium group of Arg221, negatively charged oxygen of sulfonate  $\text{O}^-$  with amide proton of Gly220 and two fluorine atoms form hydrogen bonds with amide protons of Ala217, Gly218. Although this compound has nearly same polar surface area (Table 3) as that of compound **7**, lack of second ionizable group seems to have contributed for four fold less inhibitor potency than compound **7** with binding energy of -46.844 kcal/mol.

#### Compound 9

Compound **9** is naphthyl  $\alpha,\alpha$ -difluorotetrazole (Table 2). In addition to the interactions of the naphthalene ring and hydrogen bonding interactions of fluorine atoms,  $\text{N}_c$  of ionized tetrazole forms hydrogen bond

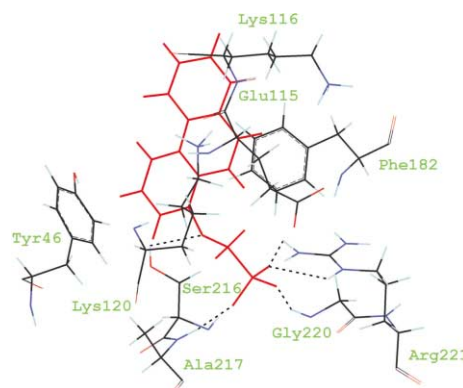


Figure 3. Binding orientation of compound **6** with PTP 1B active site

Table 3. Solvent accessible surface area calculations ( $\text{\AA}^2$ ) for compounds **1–16** and PTP 1B enzyme

Compd	Polar surface area ( $\text{\AA}^2$ )	Non polar surface area ( $\text{\AA}^2$ )	Total solvent accessible surface area ( $\text{\AA}^2$ )	Total enclosed volume ( $\text{\AA}^3$ )
1	142	236	378	563 $\pm$ 1.3
2	231	246	477	748 $\pm$ 4.3
3	283	343	626	1028 $\pm$ 0.3
4	148	293	436	686 $\pm$ 4.2
5	148	300	448	700.3 $\pm$ 3.3
6	143	355	498	809.7 $\pm$ 0.3
7	121	317	438	708.7 $\pm$ 1.0
8	124	311	435	707.3 $\pm$ 5.7
9	113	330	443	710.5 $\pm$ 4.5
10	87	330	417	663 $\pm$ 2.2
11	162	297	459	459 $\pm$ 2.9
12	113	374	487	822.4 $\pm$ 3.9
13	118	373	491	827.6 $\pm$ 1.8
14	110	389	499	828.1 $\pm$ 5.2
15	79	391	470	781.7 $\pm$ 5.3
16	159	359	518	867.6 $\pm$ 4.4
PTP 1B Enzyme	3993	8573	12530	58502 $\pm$ 1.1

with guanidium group of Arg221, N<sub>d</sub> with amide proton of Gly220. This compound has slightly less polar surface area compared to compound **7** and showed 4-fold less inhibitor potency than compound **7** with binding energy of  $-49.385$  kcal/mol.

### Compound 10

Compound **10** is naphthyl  $\alpha,\alpha$ -difluorocarboxylate (Table 2). In addition to the interactions of naphthalene ring and hydrogen bonding interactions of two fluorine atoms, the C=O of carboxylate forms hydrogen bond with guanidium group of Arg221, O<sup>-</sup> with amide proton of Gly220. This compound has less polar surface area among the series of naphthyl  $\alpha,\alpha$ -difluorophosphate and biosteres (Table 3). Hence this compound showed ten fold less inhibitor potency than compound **7** with binding energy of  $-31.607$  kcal/mol.

### Compound 11

Compound **11** is naphthyl OCF-malonoate (Table 2). This compound maximized hydrogen bond interactions of its OCF-malonoate group in a manner similar to difluorophosphate group. First carboxylate group C<sub>1</sub>=O form two hydrogen bonds with guanidium group of Arg221, O<sub>a</sub><sup>-</sup> with amide proton of Gly220, second carboxylate group C<sub>2</sub>=O with amide proton of Gly218, O<sub>b</sub><sup>-</sup> with amide proton of Ser216, F with amide proton of Ala217. The extensive hydrogen bonding network formed by this compound force the naphthyl moiety to move away from the surface of signature motif. This

movement prevented naphthyl moiety to make favorable interactions with the residues present at the cleft of signature motif. Because of extensive hydrogen bonding network this compound showed better binding energy but the entropic cost resulted in less inhibitory potency. This is evident from the high polar surface area and less nonpolar surface area (Table 3) of this compound in the naphthyl  $\alpha,\alpha$ -difluoro phosphate and its biosteres. Hence this compound is less active than sulfonate (**8**) and tetrazole (**9**) biosteres (Table 2).

## Biphenyl $\alpha,\alpha$ -Difluoro Phosphate and Biosteres

### Compound 12

Compound **12** is biphenyl  $\alpha,\alpha$ -difluorophosphate (Table 2) with high activity among the series of biphenyl  $\alpha,\alpha$ -difluoro phosphate and biosteres. The biphenyl ring system of this compound exhibited hydrophobic  $\pi$ - $\pi$  interactions with Tyr46, Phe182, van der Waals contacts with aliphatic side chains of Glu115, Lys116, Lys120, Val49, Ala217, Ile219, strong cationic  $\pi$ -interaction with side chain NH<sub>3</sub><sup>+</sup> of Lys116, Lys120. The difluoro phosphate group exhibited hydrogen bond interactions with signature motif residues. The two fluorine atoms form hydrogen bonds with amide protons of Phe182, Ala217, P=O with guanidium group of Arg221, O<sub>a</sub><sup>-</sup> with amide proton of Gly218, O<sub>b</sub><sup>-</sup> with amide proton of Gly220.

This compound exhibited 2-fold more inhibitor potency than naphthyl  $\alpha,\alpha$ -difluorophosphate (**7**). The strong cationic  $\pi$ -interactions of biphenyl ring system with side chain NH<sub>3</sub><sup>+</sup> of Lys116, Lys120 and van der Waals contacts with side chain of Glu115, Lys116, Lys120 have contributed for the enhanced inhibitory activity. This compound shows high polar surface area (Table 3), inhibitory activity among the series of biphenyl  $\alpha,\alpha$ -difluorophosphate and its biosteres with binding energy of  $-66.196$  kcal/mol.

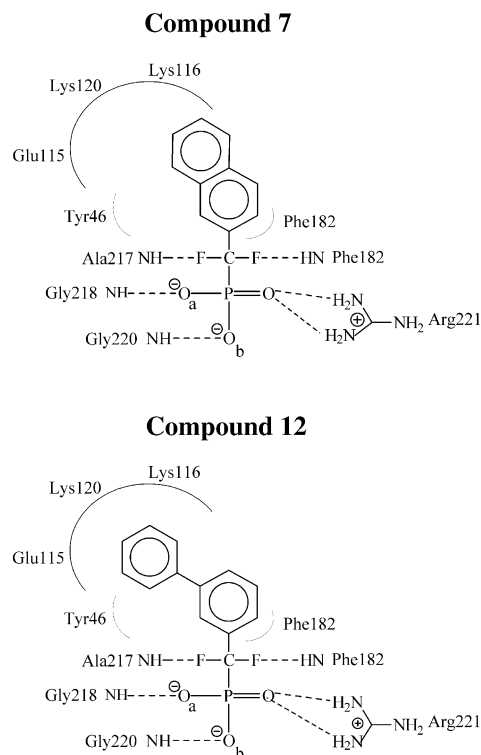


**Figure 4.** Schematic representation of interactions between compound **7** and **12** with PTP 1B active site residues.

**Table 4.** Binding orientation data of inhibitors with PTP 1B enzyme

Compd	$E_{\text{bind}}^a$	Rmsd <sup>b</sup>	Number of hydrogen bonds
<b>1</b>	$-21.677$	1.11	4
<b>2</b>	$-54.110$	1.04	5
<b>3</b>	$-85.577$	1.00	9
<b>4</b>	$-48.147$	1.05	5
<b>5</b>	$-49.498$	1.97	5
<b>6</b>	$-52.682$	1.94	4
<b>7</b>	$-64.830$	1.60	5
<b>8</b>	$-46.844$	1.47	4
<b>9</b>	$-49.385$	1.25	4
<b>10</b>	$-31.607$	0.92	4
<b>11</b>	$-56.182$	1.17	6
<b>12</b>	$-66.196$	1.48	5
<b>13</b>	$-47.822$	1.23	5
<b>14</b>	$-46.018$	1.29	4
<b>15</b>	$-23.090$	1.20	5
<b>16</b>	$-55.654$	1.48	6

<sup>a</sup> $E_{\text{bind}}$  is energy of binding =  $E_{\text{complex}} - (E_{\text{enzyme}} + E_{\text{inhibitor}})$  (kcal/mol).

<sup>b</sup>Rmsd rms deviation of active site residues (all atoms) compared to the refined enzyme structure.

### Compound 13

Compound **13** is biphenyl  $\alpha,\alpha$ -difluorosulphonate (Table 2), maintained hydrophobic, van der Waals contacts, cationic  $\pi$  interactions, aromatic  $\pi$ – $\pi$  stack interactions of biphenyl ring system, and the hydrogen bond interactions of two fluorine atoms same as that of compound **13**. The  $\text{S}=\text{O}_a$  forms hydrogen bond with guanidium group of Arg221,  $\text{S}=\text{O}_b$  with amide proton of Gly220,  $\text{O}^-$  with amide proton of Ala217. Compound **13** has nearly same polar surface area as that of compound **12**, and 7-fold less potent than compound **12** due to lack of second ionizable group. This compound binds to PTP 1B active site with binding energy of  $-47.822$  kcal/mol.

### Compound 14

Compound **14** is biphenyl  $\alpha,\alpha$ -difluorotetrazole (Table 2). It has maintained all the interactions of biphenyl ring system and hydrogen bonding interactions of two fluorine atoms same as that of compound **12**.  $\text{N}_a$  of ionized tetrazole forms hydrogen bond with amide proton of Gly220,  $\text{N}_b$ ,  $\text{N}_c$  with guanidium side chain of Arg221,  $\text{N}_d$  with amide proton of Gly218. This compound showed nearly same polar surface area (Table 3) as that of compound **12** and is 4 times less potent than compound **12**. This compounds binds to the active site of PTP 1B with binding energy of  $-46.018$  kcal/mol.

### Compound 15

Compound **15** is biphenyl  $\alpha,\alpha$ -difluorocarboxylate (Table 2). The interactions of biphenyl ring system and hydrogen bonding interactions of two fluorine atoms were same as that of compound **12**. The  $\text{C}=\text{O}$  of this compound form hydrogen bond with guanidium group of Arg221,  $\text{O}^-$  with amide proton of Gly220. Compound **15** possesses less polar surface area (Table 3) and less inhibitor potency with binding energy of  $-23.090$  kcal/mol among the series of biphenyl  $\alpha,\alpha$ -difluorophosphate and biosteres.

### Compound 16

Compound **16** is biphenyl OCF-malonoate (Table 2). First carboxylate group  $\text{C}_1=\text{O}$  forms hydrogen bond with amide proton of Gly220,  $\text{O}_a^-$  with amide proton of Ser216, second carboxylate group  $\text{C}_2=\text{O}$  forms two hydrogen bonds with guanidium group of Arg221,  $\text{O}_b^-$  with amide proton of Gly218, F with amide proton of Ile219, etherial oxygen with amide proton of Ala217, with binding energy of  $-55.654$  kcal/mol. Solvent accessible surface area calculations indicate that this compound has high polar surface area (Table 3) which is evident from extensive hydrogen bonding interactions. Because of extensive hydrogen bonding network the orientations of the biphenyl ring system is changed and prevented this compound to form favorable contacts with the residues present at the cleft of signature motif. Hence this compound showed less inhibitor potency than compounds **13**, **14**.

### Discussion

Docking studies and subsequent molecular dynamics simulations for a series of aryloxymethylphosphonates revealed the factors responsible for their inhibitory potency and binding orientations. Docking and dynamics simulations on benzylic  $\alpha,\alpha$ -difluoro phosphate and its biosteres resulted in the identification of effective monoanionic phosphate biosteres.

#### Aryloxymethylphosphonates

Molecular recognition and subsequent interaction of inhibitors with PTP 1B enzyme active site residues occur through hydrogen bonding interactions. These specific hydrogen bonds appear to be anchoring points for these inhibitors. The potency of the inhibitors is mainly governed by the hydrophobic interactions, cationic  $\pi$  stacking interactions, van der Waals contacts of the inhibitors with the residues present at the cleft of signature motif in addition to hydrogen bonding interactions.

Compound **2** with propionate side chain forms hydrophobic, cationic  $\pi$  interactions and hydrogen bond interactions with Lys120 residue in addition to the interactions of compound **1**, showed 3-fold more inhibitor potency than compound **1**. The naphthalene ring of compounds **4** and **5** exhibited hydrophobic, cationic  $\pi$  stacking interactions, van der Waals contacts with Glu115, Lys116, Lys120 residues that are not possible for compound **1**. Hence, compounds **4** and **5** with naphthalene ring system are three fold more potent than compound **1**. Compound **2** with aliphatic side chain and terminal carboxyl group, compounds **4** and **5** with naphthalene ring showed nearly same inhibitor potency. In the case of compound **2**, charged interaction and hydrogen bonding interaction of propionate group with Lys120 contributed for the activity. In the case of compounds **4** and **5**, naphthyl ring system forms cationic  $\pi$  interactions with side chain  $\text{NH}_3^+$  of Lys120, van der Waals contacts with side chains of Glu115, Lys116, Lys120 contributed for the activity of compounds **4** and **5**. Compound **6** with phenanthrene ring system as aryl substituent of aryloxymethylphosphate group showed 8-fold more inhibitor potency than compound **1**. The terminal phenyl ring of phenanthrene ring system form cationic  $\pi$  interactions with side chain  $\text{NH}_3^+$  of Lys116 in addition to the charged interactions with Lys120, van der Waals contacts with Glu115, Lys116, Lys120. These additional interactions with high nonpolar surface area as evident from surface area calculations have contributed for 8-fold more inhibitor potency of this compound than compound **1**.

Compounds **1**, **2**, **4**, **5**, and **6**, showed similar modes of binding in the active site of PTP 1B. Orientation of these inhibitors in enzyme active site indicates that in addition to the hydrogen bonding interactions with signature motif residues, inhibitors having properly oriented functional groups which can interact with residues present at the cleft of signature motif (Glu115, Lys116, Lys120) by hydrophobic, cationic  $\pi$  interactions, van der Waals contacts may show enhanced inhibitor potency.



Compound **3** has highest activity among aryloxymethylphosphonates, which can be interpreted from its high interaction energy ( $E_{\text{bind}}$ ). This compound exhibited different binding mode with active site of PTP 1B. Having high total enclosed volume, compound **3** occupied effectively the hydrophobic pocket formed by Tyr46, Arg47, Asp48, Val49. Additional hydrogen bonds, hydrophobic interactions charged interactions, and van der Waals contacts of second phenyloxymethylphosphonate with the residues of the hydrophobic pocket (Tyr46, Arg47, Asp48, Val49) contributed significantly toward enhanced inhibitor activity of compound **3**.

The X-ray crystal structure of bis (*para*-phosphonophenyl) methane (BPPM), a synthetic high affinity low molecular weight non peptidic substrate with PTP 1B<sup>23</sup> reveals that one half of the phosphonophenyl methane moiety (proximal half) occupies the canonical site (active site), and second half of phosphonophenyl methane moiety (distal half) occupies a different site in the vicinity of active site.

Proximal half phosphonophenyl methane of BPPM engaged in electrostatic, hydrogen bonding interactions with Arg221, amide protons of Ser216-Arg221, van der Waals contacts with aliphatic side chains, and aromatic  $\pi$ - $\pi$  stacking interactions with Tyr46 and Phe182 residues. In case of compound **3** (Table 1), which belongs to bis (*para*-oxymethylphosphonophenyl) methane the phenyl ring A (Table 1), exhibited electrostatic interaction with Arg221, hydrogen bonding with Arg221, Ser216, Ala217, Gly218 (Fig. 3). Phenyl ring exhibited aromatic  $\pi$ - $\pi$  stacking interactions with Tyr46 and Phe182, van der Waals contacts with side chains of Ser216, Ala 217, Gly218.

Distal half phosphonophenyl methane of BPPM makes aromatic  $\pi$ - $\pi$  stacking interactions with Phe182, and hydrogen bonding with Gln262 residue. In the case of compound **3** the phenyl ring B (Table 1) occupied the hydrophobic pocket formed by the Tyr46, Arg47, Asp48, Val49 residues. This phenyl ring made hydrophobic contacts with side chain of Arg47, Asp48, Val49, charged interaction with Arg47, hydrogen bonding interactions with Arg47, Asp48, and Val49.

In BPPM, the spacer methyl group makes van der Waals contacts with the carbonyl oxygen of Asp48 and the side chain of Val49. The spacer group in compound **3** makes hydrophobic contacts with Ala217.

Although BPPM and compound **3** have similar structures, because of the methylene bridge between etherial oxygen and phosphonate group of compound **3** (Table 1), the phenyl ring (B) binds to the hydrophobic pocket (Tyr46, Arg47, Asp48, Val49). Our molecular modeling results are comparable to the X-ray crystal structure of BPPM.

In general, the activity of the compounds in this series not only depends on the hydrogen bond interactions of the inhibitors with signature motif residues but also the

interactions of the properly oriented functional groups of the inhibitors with residues present at the cleft of signature motif of PTP 1B enzyme active site.

### Benzylic $\alpha,\alpha$ -difluorophosphate and biosters

This series includes  $\alpha,\alpha$ -difluorophosphate, sulfonate, tetrazole (ionized), carboxylates, attached to naphthyl/biphenyl ring system. The polar surface area of sulfonate and tetrazole is closer to phosphate group (Table 3). Even though sulfonate and tetrazole biosteres are not able to form the additional hydrogen bonds of second ionizable oxygen  $O_2^-$  of phosphate group (**7**, **11**), due to similar polar surface area, compounds **8**, **9**, **13**, and **14** (Table 2) bearing these two functional groups exhibited more activity than other biosteres.

Compounds **10** and **15** (Table 2) bearing carboxylate functional group showed poor inhibitor potency and energy of binding. Poor inhibitor activity of these compounds can be explained from the less polar surface and less number of hydrogen bonds compared to phosphate group. Hence, carboxylate functional group is not a suitable biostere for phosphate group.

Compounds **11** and **16** (Table 2) bearing -OCF-malonoate functional group as phosphate biosteres possess high polar surface area among this series of compounds (Table 3). The malonate functional group form extensive hydrogen bond network with signature motif residues. Due to extensive hydrogen bond network benzyl ring system orientation is changed with respect to the critical residues present at the cleft of signature motif (Glu115, Lys116, Lys120). The changed orientation of these compounds prevented favorable hydrophobic, cationic  $\pi$  interactions, van der Waals contacts make these compounds poor inhibitors than sulfonate and tatrazone biosteres. Hence -OCF-malonoate functional group is not a suitable biostere for phosphate.

Among the naphthalene and biphenyl ring systems attached to  $\alpha,\alpha$ -difluoro phosphate and biosteres, compounds bearing biphenyl ring system showed comparatively more inhibitor potency than naphthalene counterparts. As the terminal phenyl ring of biphenyl ring system exhibited strong cationic  $\pi$  interactions with side chain  $NH_3^+$  of Lys 116, which was not possible in naphthalene ring system (Fig. 4). These additional interactions contributed for the enhanced activity of the compounds with biphenyl ring system. This is evident from surface area calculations (Table 3) that compounds bearing biphenyl ring system possess more nonpolar surface area than naphthalene ring system.

The X-ray crystal structure of difluoronaphthylmethyl phosphonic acid with PTP 1B<sup>24</sup> revealed that the naphthalene ring of this compound forms close aromatic  $\pi$ - $\pi$  stacking interactions with Phe182 than Tyr46. Compound **7** belongs to naphthyl  $\alpha,\alpha$ -difluorophosphate and biosteres (Table 2) exhibited similar aromatic  $\pi$ - $\pi$  stacking interactions with Phe182 than Tyr46 of PTP1B (Figure 4). This indicates that the binding mode of



compound **7** obtained from our molecular modeling study is similar to the X-ray crystal structure of difluoronaphthylmethyl phosphonic acid with PTP 1B.

Compounds bearing biphenyl ring system and sulfonate, tetrazole functional groups showed comparatively good activity than other compounds. Hence, sulfonate and tetrazole functional groups can be incorporated as phosphate biosteres in further design of PTP 1B inhibitors. These findings are supported by surface area calculations and are in agreement with inhibitor potency of the compounds.

### Conclusions

By docking and three-dimensional structure of PTP 1B we have deduced reasonable binding model and factors responsible for inhibitor potency for aryloxymethyl phosphonates. Analysis of dynamics trajectories revealed that:

- i. Hydrogen bonding interactions of oxymethylphosphonate group with signature motif residues of PTP 1B serve as molecular recognition elements for inhibitory activity.
- ii. The hydrophobic residues present at the cleft of signature motif (Glu115, Lys116, Lys120) govern the inhibitor potency of compounds **2**, **4**, **5** and **6** (Table 1). Because of the additional interactions of propionate side chain, compound **2** exhibited better activity than compound **1**. Compounds **4**, **5**, and **6** showed more inhibitor potency due to their increased hydrophobic character. Among these compounds compound **6** with high nonpolar surface area showed highest inhibitor activity.
- iii. Compound **3** (Table 1) belongs to bis(para-oxymethylphosphonophenyl) methane type showed different binding mode. The second phenyloxymethylphosphate of compound **3** effectively occupied the hydrophobic pocket formed by Tyr46, Arg47, Asp4, Val49 residues of PTP 1B contributed for high inhibitor potency. This compound binds to PTP 1B active site predominantly by hydrophobic interactions and hydrogen bond binding interactions possesses highest activity among aryloxymethylphosphonates.
- iv. From hydrogen bond interactions and surface area calculations on a series of naphthyl/biphenyl  $\alpha,\alpha$ -difluoro phosphate and isosteres, we have identified sulfonate and tetrazole functional groups as effective monoanionic biosteres for phosphate group. Due to strong hydrophobic, cationic  $\pi$  interactions of terminal phenyl ring of biphenyl ring system with Glu115, Lys116, Lys120 amino acid residues of PTP 1B, biphenyl ring system was found to be more suitable aromatic functionality than naphthalene ring system.
- v. The molecular modeling results of compounds **3** and **7** are compared with the available X-ray structures of the related compounds.
- vi. Biological activity of the inhibitors in the present study was found to be quite consistent with molecular modeling results.

## Experimental

### Molecular modeling

Molecular modeling operations were performed using SYBYL 6.6<sup>25</sup> running on Silicon Graphics Indy R5000 workstation. All the minimizations and MD simulations were performed using Tripos force field.<sup>26</sup> Solvent accessible surface area calculations were performed using the molecular modeling package QUANTA 4.0, (1993).<sup>27</sup>

### Enzyme structure

The starting enzyme structure of PTP 1B (PDB entry 1ecv) was obtained from the Protein Data Bank of Brookhaven National Laboratory. All the crystal waters were retained, hydrogens were added and enzyme structure was subjected to a refinement protocol<sup>28</sup> in which the constraints on the enzyme were gradually removed and minimized until the root mean square deviation was 0.01 kcal/mol Å. The energy minimized structure was used for docking studies.

### Inhibitors

A series of aryloxymethylphosphonates<sup>18</sup> with PTP 1B enzyme inhibitory activity  $K_i$  (mM) are reported in Table 1. A series of  $\alpha,\alpha$ -difluoro benzylic phosphate and its biosteres<sup>19</sup> with PTP 1B inhibitory activity  $IC_{50}$  ( $\mu$ M) are reported in Table 2. The inhibitors were built from the SYBYL fragment library. Energy minimization was performed using Powell optimization method; with a convergence of 0.001 kcal/mol Å. Charges were calculated by Gasteiger–Hückel method. Simulated annealing was then performed. The system was heated at 1000 K for 1.0 ps and then annealed to 250 K for 1.5 ps. The annealing function was exponential; 50 such cycles of annealing were run and those resulting 50 conformers were optimized using the methods described above. The lowest energy conformer was selected for docking and MD simulations. All the inhibitors were modeled in their ionic forms.

### Docking and molecular dynamics simulations

The docking and MD simulations were carried out on PTP 1B enzyme for each inhibitor. Active site was defined using 12 Å radius around the inhibitor and MD simulations were performed on the active site with rest of the enzyme fixed. Each compound was docked into the active site using crystal ligand as a template for initial placement. The compound was moved and/or rotated to reduce the bumps. The non-bonded interaction energy between the inhibitor and the protein, both electrostatic and van der Waals forces was evaluated using SYBYL/Interactive docking to find the low energy binding orientations. To optimize enzyme–inhibitor interactions inhibitor was fixed in low energy orientation and the initial model was minimized using the steepest descent method until the gradient convergence was less than 1 kcal/mol Å. The system was then minimized using Powell method to a maximum gradient of 0.01 kcal/mol Å. The structure obtained

from energy minimization was subjected to MD simulations at 300 K with equilibration for 10 ps, followed by simulation for 45 ps with a time step of 1 fs, using NTV ensemble. Trajectory frames were collected after every 100 steps. A constant dielectric of 1.0 and non-bonded cut off of 8 Å was used throughout the calculations. A set of trajectory frames were selected on the basis of potential energy, hydrogen bond interactions, orientation of the inhibitors within the active site for further studies. These selected trajectory frames were minimized until rms of 0.01 kcal/mol Å was reached.

### Surface area calculations

Solvent accessible surface area calculations (Table 3) indicate that non-polar surface area of all the inhibitors is higher than the polar surface area. The hydrophobic surface area of PTP 1B being high, the active site of this enzyme demand inhibitors, which possess more hydrophobic character.<sup>29</sup>

### Acknowledgements

The authors thank University Grants Commission, New Delhi for financial support under the Special Assistance Program and COSIST. One of the authors (S.M.V) thanks University Grants Commission (UGC) for a Senior Research Fellowship. S.M.V. also thank Dr. V.M. Gokhale and Pranav Kumar S. K for useful discussions.

### References and Notes

- Drake, P. G.; Posner, B. I. *Mol. Cell. Biochem.* **1998**, *182*, 79.
- White, M. F.; Khan, C. R. *J. Biol. Chem.* **1994**, *269*, 1.
- Byon, J. C. H.; Kusari, A. B.; Kusari, J. *Mol. Cell. Biochem.* **1998**, *182*, 101.
- Ahmad, F.; Li, P.-M.; Meyerovitch, J.; Goldstein, B. J.; Chernoff, J.; Gustafson, T. A.; Kusari, J. *J. Biol. Chem.* **1995**, *270*, 20503.
- Bandyopadhyay, D.; Kusari, A.; Kenner, K. A.; Liu, F.; Chernoff, J.; Gustafson, T. A.; Kusari, J. *J. Biol. Chem.* **1997**, *272*, 1639.
- Kusari, J.; Kenner, K. A.; Shu, K.-I.; Hill, D. E.; Henry, R. R. *J. Clin. Invest.* **1994**, *93*, 1156.
- Ahmad, F.; Lonsidane, R. V.; Bauer, T. L.; Ohannesian, J. P.; Marco, C. C.; Goldstein, B. J. *Metabolism* **1997**, *46*, 1140.
- Elchelby, M.; Payette, P.; Michaliszyn, E.; Cromlish, W.; Collinschan, C. C.; Ramachandran, C.; Gresser, M. J.; Tremblay, M. L.; Kennedy, B. P. *Science* **1999**, *283*, 1544.
- Burke, T. R., Jr.; Kole, H. K.; Roller, P. P. *Biochem. Biophys. Res. Commun.* **1994**, *204*, 129.
- Montserat, J.; Chen, L.; Lawrence, D. S.; Zhang, Z.-Y. *J. Biol. Chem.* **1996**, *271*, 7868.
- Kole, H. K.; Smyth, M. S.; Rubs, P. L.; Burke, T. R., Jr. *Biochem. J.* **1995**, *311*, 1025.
- Chen, L.; Wu, L.; Otaka, A.; Smyth, M. S.; Roller, P. P.; Burke, T. R., Jr. *Biochem. Biophys. Res. Commun.* **1995**, *216*, 976.
- Inoue, A.; Kawai, T.; Wakita, M.; Iimura, Y.; Sugimota, H.; Kawakami, Y. *J. Med. Chem.* **1996**, *39*, 4460.
- Hariprasad, V.; Kulkarni, V. M. *J. Mol. Mod.* **1997**, *3*, 443.
- Furet, P.; Carayatti, G.; Lydon, N.; Priestle, J. P.; Sowadski, J. M.; Trinks, U.; Traxler, P. J. *J. Comput.-Aided. Mol. Des.* **1995**, *9*, 465.
- Winter, H. D.; Herdewijn, P. *J. Med. Chem.* **1996**, *39*, 4727.
- Gokhale, V. M.; Kulkarni, V. M. *J. Comput.-Aided. Mol. Des.* **2000**, *14*, 495.
- Ibrahimi, O. A.; Wu, L.; Zhao, K.; Zhang, Z.-Y. *Bioorg. Med. Chem. Lett.* **2000**, *10*, 457.
- Kotoris, C. K.; Chen, M. J.; Taylor, S. D. *Bioorg. Med. Chem. Lett.* **1998**, *8*, 3275.
- Zhang, Z.-Y. *CRC. Crit. Rev. Biochem. Mol. Biol.* **1998**, *33*, 1.
- Sarmeinto, M.; Wu, L.; Keng, Y. F.; Song, L.; Luo, Z.; Haung, Z.; Wu, G. Z.; Yaun, A. K.; Zhang, Z. Y. *J. Med. Chem.* **2000**, *43*, 146.
- Yamaoti, Y.; Ishihara, Y.; Kuntz, I. D. *J. Med. Chem.* **1994**, *37*, 3141.
- Puius, Y. A.; Zhao, Y.; Sullivan, M.; Lawrence, D. S.; Almo, S. C.; Zhang, Z.-Y. *Proc. Natl. Acad. Sci. U.S.A.* **1997**, *94*, 13420.
- Groves, M. R.; Yao, Z.-J.; Roller, P. P.; Burke, T. R., Jr.; Barford, D. *Biochemistry* **1998**, *37*, 17773.
- SYBYL 6.6 molecular modeling software available from Tripos Associates Inc., 1699, St Hanley Road, St. Louis, MO 63144-2913, USA.
- Clark, M.; Crammer, R. D. *J. Comput. Chem.* **1989**, *10*, 982.
- QUANTA (version 4.0) (1994) Molecular Simulations Inc. 9685 Scranton Road, San Diego, CA 92121-3752, USA.
- Levit, M.; Lifson, S. *J. Mol. Biol.* **1969**, *46*, 269.
- Isbister, B. D.; St. Hilaire, P. M.; Toone, E. J. *J. Am. Chem. Soc.* **1995**, *117*, 12877.